

Suzaku investigation into the nature of the nearest ultraluminous X-ray source, M33 X-8.

Naoki ISOBE¹, Aya KUBOTA², Hiroshi SATO², and Tsunefumi MIZUNO³

¹*Institute of Space and Astronautical Science (ISAS), Japan Aerospace Exploration Agency (JAXA)
3-1-1 Yoshinodai, Chuo-ku, Sagami-hara, Kanagawa 252-5210, Japan
n-isobe@ir.isas.jaxa.jp*

²*Department of Electronic Information Systems, Shibaura Institute of Technology,
307 Fukasakum Minuma-ku, Saitama-shi, Saitama, 337-8570, Japan*

³*Department of Physics, Hiroshima University, 1-3-1 Kagamiyama, Higashi-Hiroshima, Hiroshima 739-8526, Japan*

(Received 2012 February 27; accepted 2012 May 20)

Abstract

The X-ray spectrum of the nearest ultraluminous X-ray source, M33 X-8, obtained by Suzaku during 2010 January 11 – 13, was closely analyzed to examine its nature. It is, by far, the only data with the highest signal statistic in 0.4 – 10 keV range. Despite being able to reproduce the X-ray spectrum, Comptonization of the disk photons failed to give a physically meaningful solution. A modified version of the multi-color disk model, in which the dependence of the disk temperature on the radius is described as r^{-p} with p being a free parameter, can also approximate the spectrum. From this model, the innermost disk temperature and bolometric luminosity were obtained as $T_{\text{in}} = 2.00_{-0.05}^{+0.06}$ keV and $L_{\text{disk}} = 1.36 \times 10^{39} (\cos i)^{-1}$ ergs s⁻¹, respectively, where i is the disk inclination. A small temperature gradient of $p = 0.535_{-0.005}^{+0.004}$, together with the high disk temperature, is regarded as the signatures of the slim accretion disk model, suggesting that M33 X-8 was accreting at high mass accretion rate. With a correction factor for the slim disk taken into account, the innermost disk radius, $R_{\text{in}} = 81.9_{-6.5}^{+5.9} (\cos i)^{-0.5}$ km, corresponds to the black hole mass of $M \sim 10 M_{\odot} (\cos i)^{-0.5}$. Accordingly, the bolometric disk luminosity is estimated to be about $80 (\cos i)^{-0.5} \%$ of the Eddington limit. A numerically calculated slim disk spectrum was found to reach a similar result. Thus, the extremely super-Eddington luminosity is not required to explain the nature of M33 X-8. This conclusion is utilized to argue for the existence of intermediate mass black holes with $M \gtrsim 100 M_{\odot}$ radiating at the sub/trans-Eddington luminosity, among ultraluminous X-ray sources with $L_{\text{disk}} \gtrsim 10^{40}$ ergs s⁻¹.

1. Introduction

A number of nearby galaxies are known to host luminous X-ray sources with an X-ray luminosity of $L_X \gg 10^{39}$ ergs s⁻¹ (e.g., Fabbiano & Trinchieri 1987; Swartz et al. 2011). They are usually referred to as ultraluminous X-ray sources (ULXs; Makishima et al. 2000). The ULXs are found to be less common in the Local Universe, as no persistent ULX is yet identified in our Galaxy and M31. In spite of significant efforts in more than three decade since their discovery, we have not yet arrived at the general conclusion on their nature.

It is widely believed from their observational features (e.g., Makishima et al. 2000) that the ULX phenomena are related to accreting black holes. Because the luminosity of an accreting black hole is thought to increase as a function of the black hole mass M and accretion rate \dot{M} on the simplest assumption, two distinct ideas are currently proposed to interpret the high X-ray luminosity of the ULXs. The first option supposes that the luminosity of the ULXs should not exceed the Eddington luminosity (L_E), as most Galactic black hole binaries meet this criterion (e.g., Kubota & Makishima 2004). As a result, the ULXs are required to harbor an intermediate-mass black holes with a mass of $M \gg 10 M_{\odot}$ with M_{\odot} being the so-

lar mass. In the second alternative, a super Eddington luminosity is permitted. Consequently, the ULXs are regarded as a stellar-mass black hole ($M \lesssim 10 M_{\odot}$), accreting at a super-critical mass accretion rate ($\dot{M} \gg L_E/c^2$ with c being the speed of light).

It is of vital importance to construct a reliable technique to gauge the mass and/or mass accretion rate of the ULXs, in order to distinguish these two conflicting interpretations. For the purpose, the dynamical mass determination is thought to provide inevitably the most stringent constraint, as is the case of the Galactic black hole binaries (e.g., Shahbaz et al. 1999; Hynes et al. 2003). However, the dynamical mass of the ULXs has remained yet to be explored.

X-ray spectra and their variability have been one of the most valuable tools to probe the properties of the ULXs. A naive inspection on the X-ray spectra in the 0.5 – 10 keV range categorizes the ULXs into two types; those with an X-ray spectrum dominated by emission from accretion disk which is approximated by the multi-color disk (MCD; Mitsuda et al. 1984; Makishima et al. 1986) model, and those exhibiting a power-law (PL) like X-ray spectrum. In addition, a growing number of ULXs are reported to make a spectral transition between the MCD-

like and PL-like states (e.g., Kubota et al. 2001b; Isobe et al. 2009). These spectral behaviors apparently resemble those of Galactic black hole binaries in the classical high/soft and low/hard states. However, several observational obstacles are known for this assumption as follows (e.g., Makishima et al. 2000; Mizuno et al. 2001). The X-ray spectrum of the MCD-like ULXs requires a flatter radial temperature distribution within the disk (e.g., Tsunoda et al. 2006) in comparison with that in the standard accretion disk (Shakura & Sunyaev 1973) which is adopted in the MCD model. The innermost disk radius R_{in} of the MCD-like ULX appears to be variable as $R_{\text{in}} \propto T_{\text{in}}^{-1}$ with T_{in} being the innermost disk temperature (e.g., Mizuno et al. 2001; Isobe et al. 2009), while the Galactic black hole binaries in the high/soft state are reported to follow a constancy of R_{in} (e.g., Ebisawa et al. 1993) which indicates that R_{in} corresponds to the last stable circular orbit of the accretion disk. The photon index of the PL-like ULXs ($\Gamma > 2$; e.g., Kubota et al. 2002; Isobe et al. 2009) tends to be larger than those of the Galactic black hole binaries in the low/hard state ($\Gamma \sim 1.5$; Tanaka 1997).

Recent progresses in observational (e.g., Kubota & Makishima 2004; Kubota & Done 2004) and theoretical (e.g., Watarai et al. 2000) studies on Galactic black hole binaries and their accretion disk, especially near the highest end of their X-ray luminosity, newly identified two spectral states called the very high and slim disk ones, in addition to the classical low/hard and high/soft states. In the very high state, the Galactic black hole binaries are reported to exhibit a steep PL spectrum with a photon index of $\Gamma \gtrsim 2.4$, which is softer than the PL component observed in the high/soft state ($\Gamma = 2 - 2.2$). The steep PL spectrum in this situation is ascribed to Comptonization of the disk photons within the hot corona surrounding the accretion disk. In contrast, when the Galactic black hole binaries become brighter than in the very high state, they are reported to enter the slim disk state in which a disk dominant X-ray spectrum with a flat disk temperature gradient was observed, in addition to an apparent anticorrelation between the innermost disk radius and temperature (Kubota & Makishima 2004). These properties are successfully explained by the theory of a slim accretion disk, where an optically-thick advection and photon trapping (Ohsuga et al. 2005) effectively work due to a high accretion rate ($\dot{M} > L_E/c^2$).

Triggered by these findings, it is proposed that the MCD-like and PL-like ULXs reside in the slim disk and very high states, respectively (e.g., Mizuno et al. 2001; Kubota et al. 2002; Tsunoda et al. 2006; Mizuno et al. 2007; Isobe et al. 2009). If this idea is systematically proved to be convincing, we will have acquired an empirical method to restrict the black hole mass of the ULXs. This is because the X-ray luminosity of the Galactic black hole binaries in these states are reported typically as $L_X = (0.3 - 1)L_E$ (e.g., Kubota & Makishima 2004; Kubota et al. 2001a). In other word, this interpretation consequently indicates that the ULXs are shining at a sub- or trans-Eddington luminosity. Independently,

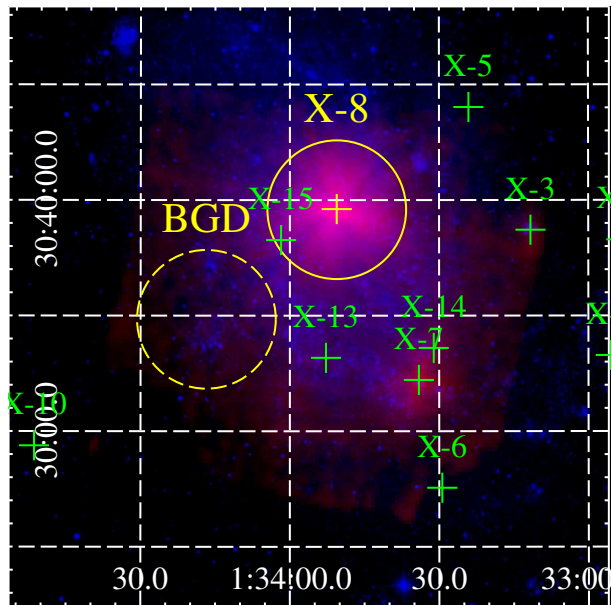


Fig. 1. Background-inclusive Suzaku XIS image in the range of 0.5 – 10 keV of M33 (red) with a bin size of $10'' \times 10''$, on which the optical image taken with the Digitized Sky Survey (blue) is superposed. The data from all the active XIS chips (XIS 0, 1 and 3; Koyama et al. 2007) were summed up. The XIS image was smoothed with a two-dimensional Gaussian kernel of a $20''$ radius, while it is not corrected for the exposure. The regions irradiated by the radioactive calibration sources at the corners of the CCD chips were removed. The X-ray sources detected with ROSAT are indicated with the green crosses, accompanied by the source name (Trinchieri et al. 1988). The XIS signals from M33 X-8 and background are integrated within the solid and dashed circles, respectively.

based on numerical simulation, Vierdayanti et al. (2008) extended to the slim accretion disk the mass estimation from the innermost disk radius, which is widely accepted for Galactic black hole binaries in the high/soft state accompanied with the standard accretion disk. It is important to confirm observationally the consistency between these techniques.

Recently, it is verified that Suzaku (Mitsuda et al. 2007) is very useful to investigate the X-ray spectral properties of the ULXs (Mizuno et al. 2007; Miyawaki et al. 2009; Isobe et al. 2008; Isobe et al. 2009). These results motivated us to perform a Suzaku observation of the nearest ULX, M33 X-8 (Trinchieri et al. 1988), in which its X-ray spectrum was obtained with the highest signal statistics in the 0.4 – 10 keV range. In the present paper, we utilized extensively the the Suzaku data of the source to investigate the nature of the ULXs.

2. Observation and Data Reduction

Within ~ 20 arcmin from the center of the nearby normal galaxy, M33, more than 10 bright X-ray sources were discovered with the Einstein observatory (Trinchieri et al. 1988). Among these sources, X-8 located near the center of the galaxy is known to show the ULX characteristics

(Makishima et al. 2000). Thanks to its proximity at a distance of 795 kpc (van den Bergh 1991), it extensively studied with the previous and active instruments including ASCA (Takano et al. 1994), BeppoSAX (Parmar et al. 2001), Chandra (La Parola et al. 2003), and XMM-Newton (e.g., Weng et al. 2009). The typical X-ray luminosity of M33 X-8, $L_X \gtrsim 10^{39}$ ergs s^{-1} , is at the lowest end of those of ULXs; only the Galactic microquasar, GRS 1915+105, is confirmed to reach occasionally such a high X-ray luminosity value (e.g., Ueda et al. 2010). Some authors claimed a flat disk temperature distribution to suggest the slim disk interpretation for the source (Foschini et al. 2006; Weng et al. 2009), although several conflicting ideas were proposed (Foschini et al. 2004; Middleton et al. 2011). These make M33 X-8 one of the most important objects to disentangle the nature of the ULXs by connecting the properties of the ULXs with those of the Galactic black hole binaries.

The Suzaku observation of M33 X-8 was performed on 2010 January 11 – 13. The X-ray imaging spectrometer (XIS; Koyama et al. 2007) and hard X-ray detector (HXD; Takahashi et al. 2007) was operated in the normal clocking mode with no window option and in the normal mode, respectively. The source was placed at the HXD nominal position of the X-ray telescope (Serlemitsos et al. 2007) above the XIS. Unfortunately, due to a significant increase in the thermal noise of the HXD PIN, the HXD effective exposure was found to reduce to only about 6.1 ks. Therefore, we concentrate on the XIS data in the present paper.

The data reduction was performed with the standard software package HEADAS 6.10. We reprocessed the XIS data with the HEADAS tool *aepipeline*, by referring to the calibration database (CALDB) as of 2011 February 10. In accordance with the standard manner, the following filtering criteria were adopted; the spacecraft is outside the south Atlantic anomaly (SAA), the time after an exit from the SAA is larger than 436 s, the geometric cut-off rigidity is higher than 6 GV, the source elevation above the rim of bright and night Earth is higher than 20° and 5° , respectively, and the XIS data are free from telemetry saturation. As a result, we derived 91.0 ks of good exposure. The XIS events with a grade of 0, 2, 3, 4, or 6 were picked up for the scientific analysis below.

3. Results

3.1. X-ray image

Figure 1 displays the 0.5 – 10 keV XIS image of M33 X-8, which is superposed on the optical image of the host galaxy taken from the digitized sky survey (Lasker et al. 1990). The brightest X-ray source in the image, detected at the center of the host galaxy, corresponds to M33 X-8. A systematic offset of $15.6''$ was noticed in the XIS coordinate determination, while it is found to be within the current systematic uncertainties (Uchiyama et al. 2008). We thus re-calibrated the XIS coordinate by ourselves, referring to the ROSAT position of M33 X-8 itself ($(\alpha_{2000}, \delta_{2000}) = (01^{\text{h}}33^{\text{m}}50^{\text{s}}58,$

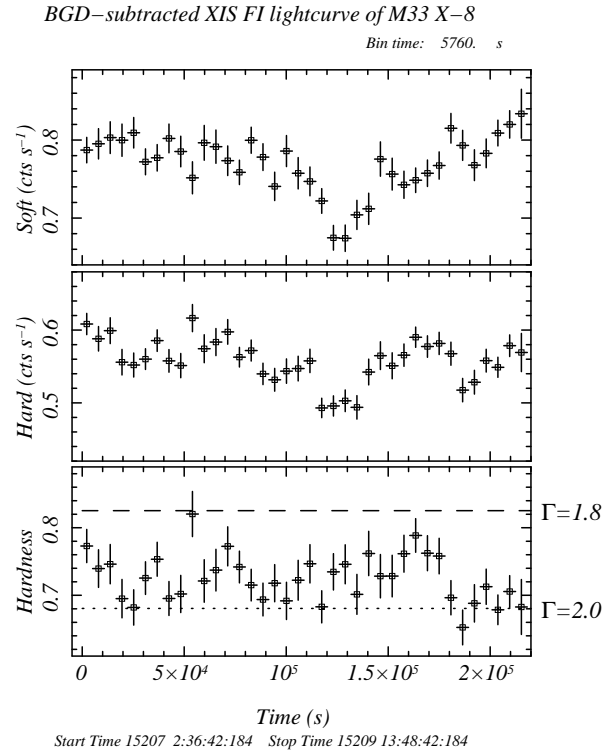


Fig. 2. Background-subtracted XIS FI lightcurve of M33 X-8. Each time bin is set to 5760 s, corresponding to the orbital period of Suzaku. The top and middle panels show the count rate in the soft (0.5 – 2 keV) and hard bands, respectively. The source hardness, simply evaluated as the hard-to-soft count-rate ratio, is shown in the bottom panel. Assuming the Galactic absorption toward M33, $N_{\text{H}} = 1.1 \times 10^{21}$ cm^{-2} (Kalberla et al. 2005), a simple PL model with a photon index of $\Gamma = 2.0$ and 1.8 corresponds to the hardness shown with the dotted and dashed lines, respectively.

$+30^{\text{d}}39^{\text{m}}36^{\text{s}}7$); Trinchieri et al. 1988). Within the XIS field of view, another X-ray source M33 X-7, a candidate of a massive spinning black hole with a mass of $M = (15.6 \pm 3.2)M_{\odot}$ (Abubekerov et al. 2010), is clearly seen at a position consistent with the ROSAT one ($(\alpha_{2000}, \delta_{2000}) = (01^{\text{h}}33^{\text{m}}34^{\text{s}}08, +30^{\text{d}}32^{\text{m}}13^{\text{s}}2$); Trinchieri et al. 1988). However, due to the insufficient signal statistics from the XIS, we regard its X-ray spectral properties as irrelevant to the scope of the present paper.

In the scientific analysis below, the XIS signals from M33 X-8 were accumulated within a solid circle in figure 1 with a $3'$ radius centered on the source, while the background level was evaluated from a source free region with the same radius, denoted by the dashed circle in figure 1. Although there is a faint ROSAT X-ray source, M33 X-15, near the edge of the source integration region, we estimated its contamination as negligible in comparison with the X-ray flux from M33 X-8 (less than 1%), based on the ROSAT result (Trinchieri et al. 1988).

3.2. X-ray lightcurve

Figure 2 shows the background-subtracted lightcurves of M33 X-8 in the soft (0.5 – 2 keV) and hard (2 – 10 keV)

Table 1. Summary of the model fitting to the XIS spectra of M33 X-8

Model	MCD	PL	MCD+PL	MCD+THCOMP	extended MCD
F_X^*	1.50	1.60	1.57	1.55	1.56
L_X^\dagger	0.57	0.83	0.75	0.65	0.71
N_H (10^{21} cm $^{-2}$)	0.0	2.38	1.80 ± 0.13	$0.85^{+0.13}_{-0.14}$	$1.47^{+0.08}_{-0.07}$
T_{in} (keV)	1.27	—	$1.38^{+0.07}_{-0.06}$	$0.36^{+0.06}_{-0.04}$	$2.00^{+0.06}_{-0.05}$
R_{in}^\ddagger	51.4	—	$29.2^{+2.5}_{-2.1}$	≤ 88.0	$81.9^{+5.9}_{-6.5}$
L_{disk}^\S	0.62	—	0.29	≤ 0.01	1.36
p	—	—	—	—	$0.535^{+0.004}_{-0.005}$
Γ	—	2.17	$2.30^{+0.08}_{-0.07}$	$1.91^{+0.04}_{-0.01}$	—
T_e (keV)	—	—	—	$1.62^{+0.10}_{-0.07}$	—
χ^2/dof	3032.7/1373	2429.7/1373	1535.8/1371	1549.6/1370	1541.8/1372

* Absorption-inclusive 0.5 – 10 keV flux in 10^{-11} ergs cm $^{-2}$ s $^{-1}$

† Absorption-corrected 0.5 – 10 keV luminosity in $10^{39}(\cos i)^{-1}$ ergs s $^{-1}$

‡ The true innermost disk radius in $(\cos i)^{-0.5}$ km. The spectral hardening factor of $\kappa = 1.7$ and the correction factor for the boundary condition of $\xi = 0.412$ are applied in the case of the MCD component, while the extended MCD model adopted $\kappa = 3$ (Watarai & Mineshige 2003) and $\xi = 0.353$ (Vierdayanti et al. 2008).

§ Absorption-corrected bolometric disk luminosity in $10^{39}(\cos i)^{-1}$ ergs s $^{-1}$, evaluated in 0.001 – 100 keV

|| The errors are omitted, because the fit was unacceptable.

bands, where the data from the two front-side illuminated (FI) CCD chips (XIS 0 and 3; Koyama et al. 2007) were summed up. The source hardness, plotted in the bottom panel of figure 2, was simply calculated as the ratio of the hard band count rate to the soft band one.

Summed over the two FI CCDs, we measured the time-averaged signal count rate of M33 X-8 as 0.77 ± 0.03 cts s $^{-1}$ and 0.56 ± 0.03 cts s $^{-1}$, respectively, in the soft and hard band. Figure 2 suggests a weak but statistically significant intensity variation ($\chi^2/\text{dof} = 145.3/37$ and $142.9/37$) during the Suzaku exposure in the soft and hard ranges with a standard deviation of 4.8% and 5.4%, respectively, around the average count rate. The hardness of the object was revealed to be relatively unchanged during the Suzaku exposure, although the source appears to exhibit a possible spectral softening near the end of the exposure.

3.3. X-ray spectrum

Since the change of hardness of M33 X-8 was suggested to be insignificant during this observation as shown in figure 2, we consider only the time-averaged spectrum of the source. Figure 3 shows the background-subtracted XIS spectrum of M33 X-8 in the range of 0.4 – 10 keV, derived with the FI and back-side illuminated (BI; XIS 1, Koyama et al. 2007) CCD chips, without removing the instrumental response. Both the FI and BI spectra were binned into energy intervals each with at least 100 events. In comparison to the previous observations with ASCA (Takano et al. 1994), BeppoSAX (Parmar et al. 2001), Chandra (La Parola et al. 2003) and XMM-Newton (e.g., Weng et al. 2009), the signal statistics of the XIS spectrum, with a total FI and BI signal counts of 1.21×10^5 and 7.47×10^4 respectively, seem to be considerably higher. The source was found to exhibit a featureless X-ray spectrum, without any clear sign of emission or absorption structure, except for instrumental and interstellar ones.

For the purpose of quantifying the spectral properties of M33 X-8, we calculated the response matrix functions for the individual CCD chips with the HEADAS tool `xisrmfgen`, while the auxiliary response files were generated by the tool `xissimarfgen` (Ishisaki et al. 2007), assuming a point source at the sky position of M33 X-8. The `xissimarfgen` tool precisely takes into account the reduction of the effective area due to contaminants on the optical blocking filters of the XIS, by referring to the appropriate version of the CALDB (see §2). We performed the spectral fitting using the version 12.6.0q of XSPEC.

As a first step, we tried to reproduce the observed XIS spectrum from M33 X-8 with an MCD model or a simple PL one. A Galactic absorption was adopted with a free hydrogen column density. These models are widely used as a standard tool for analyzing the X-ray spectra of Galactic black hole binaries and ULXs. As summarized in table 1, both models were found to be unacceptable ($\chi^2/\text{dof} = 3032.7/1373$ and $2429.7/1373$ for the MCD and PL models, respectively). The residual spectra with the MCD and PL models, shown in panels (b) and (c) of figure 3 respectively, suggest that the observed X-ray spectrum of the source seems less convex than the MCD model, while it is more convex than the simple PL model.

As a more sophisticated description for the X-ray spectrum from an accretion disk, the BHSPEC model (Davis et al. 2005)¹ was fitted to the XIS data. The model assumes a fully relativistic accretion disk around a spinning black hole, and self-consistently considers the vertical structure and radiative transfer within the disk. The disk spectrum was simulated for two representative values of the viscosity parameter, $\alpha = 0.1$ and 0.01. There are following four free parameters in the model; the black hole mass M , disk luminosity L_{disk} , disk inclination angle i

¹ This model is available in the form compatible with XSPEC from the following web <http://heasarc.gsfc.nasa.gov/docs/xanadu/xspec/models/bhspec.html>

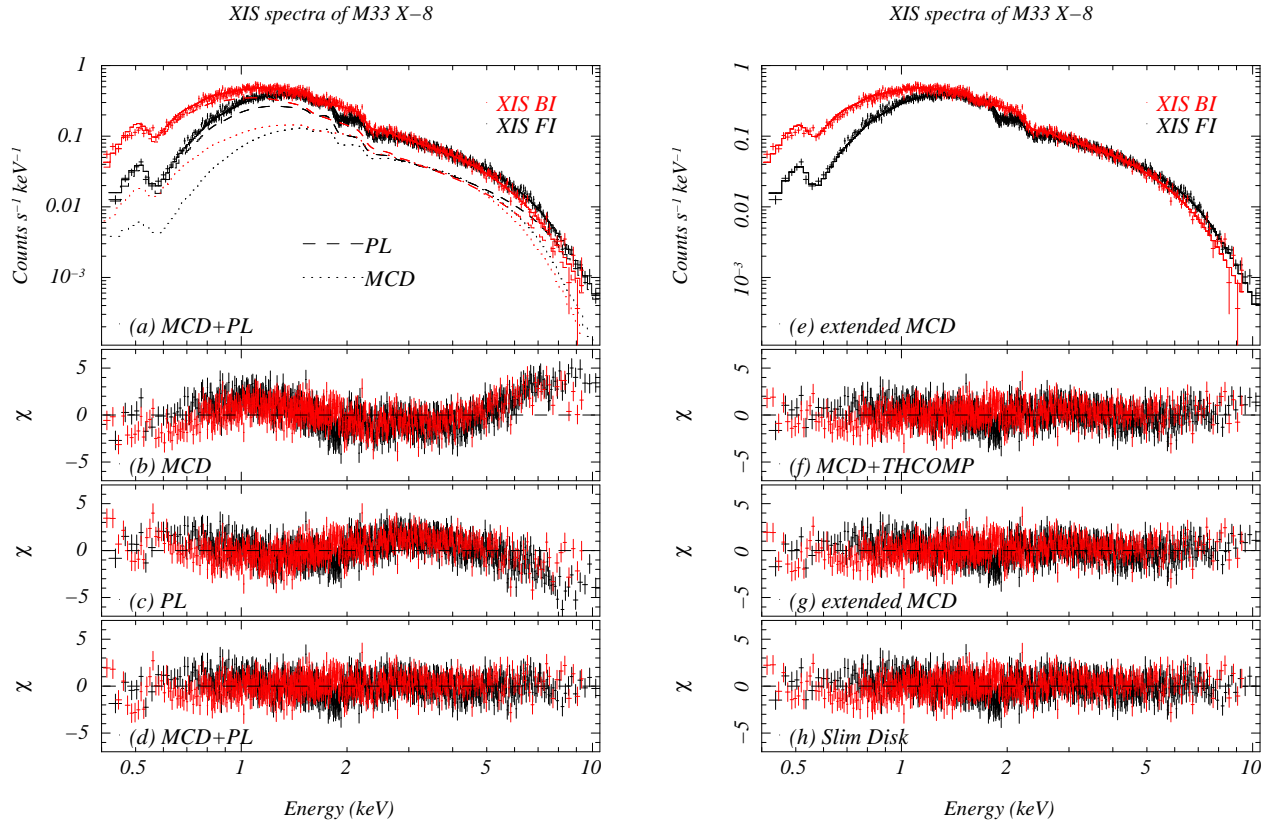


Fig. 3. Background-subtracted XIS spectrum of M33 X-8, shown without removing the instrumental response. Panels (a) and (e) compares the XIS data with the best-fit MCD+PL and extended MCD models, respectively. The residuals are displayed for (b) the best-fit MCD, (c) PL, (d) MCD+PL, (f) MCD+THCOMP, (g) extended MCD, and (h) slim disk (Kawaguchi 2003) models, respectively.

(the face-on configuration corresponds to $i = 0$), and dimensionless spin parameter a . Table 2 tabulates the resultant parameters. Although the fit was slightly improved by the BHSPEC model for $\alpha = 0.1$ ($\chi^2/\text{dof} = 2118.6/1371$) in comparison with the MCD or PL model, it was still inadequate for interpreting the XIS spectrum of M33 X-8.

Next, we examined a combination of an MCD component and a PL one (MCD+PL), both of which are subjected to a common free absorption. As shown in panels (a) and (d), a reasonable fit was derived by the model ($\chi^2/\text{dof} = 1535.8/1371$) with the spectral parameters listed in table 1. We obtained the absorption-inclusive observed X-ray flux as 1.57×10^{-11} ergs $\text{s}^{-1} \text{cm}^{-2}$ in 0.5 – 10 keV. The absorption column density, $N_{\text{H}} = (1.80 \pm 0.13) \times 10^{21} \text{ cm}^{-2}$, became higher by a factor of 1.7 than the Galactic value ($N_{\text{H}} = 1.1 \times 10^{21} \text{ cm}^{-2}$; Kalberla et al. 2005). By extrapolating the best-fit MCD component to the 0.001 – 100 keV range, we estimated the absorption-corrected bolometric disk luminosity as $L_{\text{disk}} = 2.9 \times 10^{38} (\cos i)^{-1}$ ergs s^{-1} . The innermost disk temperature of the MCD component was determined as $T_{\text{in}} = 1.38^{+0.07}_{-0.06}$ keV. The apparent innermost disk radius is evaluated as $r_{\text{in}} = 24.6^{+2.0}_{-1.8} (\cos i)^{-0.5}$ km, based on the equation $L_{\text{disk}} = 4\pi\sigma r_{\text{in}}^2 T_{\text{in}}^4$ (Mitsuda et al. 1984; Makishima et al. 1986) where σ is the Stefan-

Boltzmann constant. By taking into account a factor ξ to correct the inner disk boundary condition and a spectral hardening factor κ representing the ratio of the color temperature to the effective one, r_{in} is converted to the true innermost disk radius as $R_{\text{in}} = \xi \kappa^2 r_{\text{in}}$ (Makishima et al. 2000). According to the standard manner for the MCD model, we adopted $\xi = 0.412$ (Kubota et al. 1998) and $\kappa = 1.7$ (Shimura & Takahara 1995). Thus, the true inner radius was evaluated as $R_{\text{in}} = 29.2^{+2.5}_{-2.1} (\cos i)^{-0.5}$ km. We measured the photon index of the PL component as $\Gamma = 2.30^{+0.08}_{-0.07}$. The best-fit model indicates a dominance of the PL component over the MCD one, except for a narrow range of 3 – 5 keV.

The PL component from the Galactic black hole binaries is thought to arise via Comptonization of the disk photons in the hot corona around the black hole and accretion disk. This motivated us to re-analyze the XIS spectrum by replacing the PL component with a thermal Comptonization continuum described by the `nthcomp` model in XSPEC (Zdziarski et al. 1999; hereafter THCOMP). The seed photons for the THCOMP component were assumed to be supplied by the MCD one. As shown in panel (f) of figure 3, this MCD+THCOMP model became acceptable ($\chi^2/\text{dof} = 1549.6/1370$), yielding the best-fit parameters tabulated in table 1. The

Table 2. Results from the BHSPEC or BHSPEC+THCOMP fitting

Model	BHSPEC *		BHSPEC+THCOMP ‡
N_{H} (10^{21} cm $^{-2}$)	0.41	0.25	$1.26^{+0.10}_{-0.19}$
M (M_{\odot})	8.51	13.0	$25.7^{+2.0}_{-1.4}$
$\cos i$	> 0.99	0.67	$0.23^{+0.07}_{-0.03}$
a †	> 0.79	0.78	$a \geq 0.77$
L_{disk} (L_{E})	0.80	0.65	$0.40^{+0.14}_{-0.01}$
α ‡	0.1	0.01	0.1
Γ	—	—	$2.21^{+0.02}_{-0.11}$
T_{seed} (keV)	—	—	$0.21^{+0.05}_{-0.04}$
T_{e} (keV)	—	—	≥ 4.5
χ^2/dof	2118.6/1371	2448.0/1371	1505.0/1367

* All the errors are omitted.

† Dimensionless spin parameter.

‡ Fixed parameter in the model.

§ The best-fit parameters are shown only for $\alpha = 0.1$.

model resulted in a full dominance of the THCOMP component in the XIS energy range, and the upper limit on the absorption-inclusive 0.5 – 10 keV flux of the MCD component was evaluated as $F_{\text{X}} = 1.4 \times 10^{-13}$ ergs cm $^{-2}$ s $^{-1}$ which corresponds to only ~ 1 % of the total X-ray flux. The disk temperature of the MCD component (i.e., the seed photon temperature) was found to be significantly lower than that in the MCD+PL model as $T_{\text{in}} = 0.36^{+0.06}_{-0.04}$ keV. We derived the asymptotic photon index and coronal electron temperature of the THCOMP component as $\Gamma = 1.91^{+0.04}_{-0.01}$ and $T_{\text{e}} = 1.62^{+0.10}_{-0.07}$ keV, respectively. On the basis of the equation

$$\tau = \sqrt{2.25 + \frac{3}{(T_{\text{e}}/511 \text{ keV})[(\Gamma + 0.5)^2 - 2.25]}} - 1.5$$

(Sunyaev & Titarchuk 1980), the combination of these two quantities indicates an optically thick corona with an optical depth of $\tau \sim 15$.

We also considered a Comptonizing corona surrounding an accretion disk around a spinning black hole by a sum of the BHSPEC and THCOMP components (BHSPEC+THCOMP). Because the BHSPEC model is not written in terms of the disk temperature, it is unable to constrain the seed photon temperature, T_{seed} , of the THCOMP component to be consistent with the peak of the BHSPEC spectrum, through the BHSPEC+THCOMP fitting procedure alone. Actually, although a statistically reasonable fit was derived by the BHSPEC+THCOMP model with T_{seed} left free (see table 2), this model got settled to a physically unacceptable situation where the spectral peak of the BHSPEC component (≥ 4.5 keV) highly surpasses the seed photon temperature ($T_{\text{seed}} = 0.21^{+0.05}_{-0.04}$ keV). In addition, we failed to reconcile the seed photon temperature with the BHSPEC peak energy, in spite of a survey on the seed photon temperature in the range of $T_{\text{seed}} = 0.3 - 2$ keV. Therefore, in the present paper, we have given up to interpret the X-ray spectrum of M33 X-8 by Comptonization of X-ray photons from an accretion disk accompanied with a spinning black

hole.

Finally, in order to investigate the possibility of the slim accretion disk, which is regarded to be important at a high mass-accretion rate, we adopted a simple extension of the MCD model, where the radial temperature distribution on the disk is described as r^{-p} with the index p being a positive free parameter (Mineshige et al. 1994). Although the model has been widely referred to as a p -free disk model, we regard this nomenclature as somewhat confusing. We, then, call it as the extended MCD model in the present paper. The model with $p = 0.75$ is identical to the simple MCD model, in which a standard accretion disk (Shakura & Sunyaev 1973) is adopted, while that with a smaller value of $0.5 < p < 0.75$, is considered to approximate phenomenologically the X-ray spectra from a slim disk (e.g., Watarai et al. 2000).

Panels (e) and (g) of figure 3 clearly visualizes that the extended MCD model reproduced the observed XIS spectrum of M33 X-8 well with a goodness of fit, $\chi^2/\text{dof} = 1541.8/1372$, similar to that of the MCD+PL or MCD+THCOMP models. A rather flat temperature profile with $p = 0.535^{+0.004}_{-0.005}$ was indicated by the model. We estimated the bolometric disk luminosity as $L_{\text{disk}} = 1.36 \times 10^{39} (\cos i)^{-1}$ ergs s $^{-1}$. The innermost disk temperature, $T_{\text{in}} = 2.00^{+0.06}_{-0.05}$ keV, was found to be higher than that in the MCD+PL model. In the similar manner as for the MCD+PL model, we obtained the apparent innermost disk radius as $r_{\text{in}} = 25.8^{+1.8}_{-2.1} (\cos i)^{-0.5}$ km. In the case of the slim disk, the spectral hardening factor is suggested to become larger than that in the standard accretion disk ($\kappa = 1.7$; see above), due to various effects including enhanced electron scattering and Comptonization (e.g., Watarai & Mineshige 2003; Kawaguchi 2003). Here, we adopt $\kappa = 3$ as a typical value for the slim disk, which was required to reconcile the observed high disk temperature of the Galactic microquasar GRS 1915+105 with the prediction from the numerical simulation on the disk at a high accretion rate (Watarai & Mineshige 2003). In addition, the boundary condition is corrected by assuming $\xi = 0.353$, which was derived by taking into ac-

count the transonic flow in the pseudo-Newtonian potential (Vierdayanti et al. 2008). These yielded the "true" disk radius as $R_{\text{in}} = 81.9_{-6.5}^{+5.9} (\cos i)^{-0.5} (\xi/0.353) (\kappa/3)^2$ km.

4. Discussion

4.1. Summary of the Suzaku observation

In the Suzaku observation conducted on 2011 January 11 – 13 with an effective exposure of 91.0 ks, we successfully acquired the X-ray spectrum of the nearest ULX, M33 X-8, with the highest signal statistics in the 0.4 – 10 keV range. During the observation, the object exhibited no significant change in its spectral hardness, with only a weak intensity variation with a standard deviation of $\sim 5\%$. Without being corrected for the absorption, the time-averaged 0.5 – 10 keV flux of the source was measured as 1.57×10^{-11} ergs $\text{s}^{-1} \text{cm}^{-2}$ (evaluated from the best-fit MCD+PL model). Re-evaluated from the previous results (Takano et al. 1994; Parmar et al. 2001; La Parola et al. 2003; Foschini et al. 2004; Weng et al. 2009; Middleton et al. 2011), its 0.5 – 10 keV flux was found to stay within a relatively narrow range of $(1.4 - 1.9) \times 10^{-11}$ ergs $\text{s}^{-1} \text{cm}^{-2}$ over nearly 16 years². Thus, the source X-ray flux during the Suzaku exposure is located in the middle of its distribution in the previous observations.

Figure 3 illustrates that the time-averaged XIS spectrum of the source was described by the MCD+PL, MCD+THCOMP, or extended MCD one, with the best-fit parameters summarized in table 1, while the single PL, MCD or BHSPEC model was found to be unacceptable. Assuming the best-fit extended MCD model, the XIS spectrum was de-convolved into the spectral energy distribution in the νF_ν form, as shown in figure 4. These results are utilized to infer the nature of M33 X-8 in the following.

4.2. Comptonization scenario

When we adopt the MCD+PL model, both the disk temperature and the PL photon index of M33 X-8, $T_{\text{in}} = 1.38_{-0.06}^{+0.07}$ keV and $\Gamma = 2.30_{-0.07}^{+0.08}$, are found to fall within the range derived in the previous results (e.g., Takano et al. 1994; Parmar et al. 2001; La Parola et al. 2003; Weng et al. 2009). Especially, the steep photon index appears to be close to those of Galactic black hole binaries in the very high state ($\Gamma \gtrsim 2.4$; e.g., Miyamoto et al. 1991; Kubota & Done 2004). Actually, the very-high-state interpretation was proposed for the source by Foschini et al. (2004), based on the XMM-Newton spectra obtained in a few occasions. However, we regard that this interpretation encounters several difficulties.

The first obstacle for the very-high-state scenario comes

² Here, we neglected several XMM-Newton observations (ObsID = 0102642001, 0141980501, and 0141980601), for which we found inconsistency of more than 20 % in the flux determination between the separate results (Foschini et al. 2004; Weng et al. 2009; Middleton et al. 2011). Even if these results are taken into account, the observed 0.5 – 10 keV flux varied by only a factor of ~ 2 in the range of $(1.1 - 2.4) \times 10^{-11}$ ergs $\text{s}^{-1} \text{cm}^{-2}$.

Table 3. Physical parameters evaluated by the Slim disk model (Kawaguchi 2003)

Parameter	Value
N_{H} (10^{21} cm^{-2})	$1.23_{-0.05}^{+0.06}$
M (M_{\odot})	$13.1_{-0.7}^{+0.8}$
\dot{M} (L_{E}/c^2)	$10.5_{-0.7}^{+0.5}$
α	0.21 ± 0.05
L_{X} (ergs s^{-1}) *	0.68×10^{39}
L_{disk} (ergs s^{-1}) †	0.94×10^{39}
χ^2/dof	1516.7/1372

The model assumes a face-on disk configuration ($i = 0$).

* Absorption-corrected 0.5 – 10 keV luminosity.

† Absorption-corrected bolometric disk luminosity evaluated in 0.001 – 100 keV.

from the high disk temperature of M33 X-8, which significantly exceeds that of Galactic black-hole binaries in the strongly Comptonized very high state ($T_{\text{in}} \ll 1$ keV), termed intermediate hard state. In the case of the Galactic black-hole binaries, such a low disk temperature in the very high state is explained by a possible disk truncation at a radius significantly larger than the last stable circular orbit (Kubota & Done 2004). Secondly, the PL dominance at energies below the disk temperature T_{in} seems quite unphysical. The PL component in the very high state is naturally predicted to exhibit a sharp low-energy cut-off below the seed photon energy, because it is basically attributed to Comptonization of disk photons within the hot corona, surrounding the black hole and accretion disk.

We tried to reconcile these inconsistencies, by replacing the PL component with the Comptonization continuum described by the THCOMP mode, where the MCD emission was assumed to provide the seed photon source. The MCD+THCOMP model has eventually arrived at a different solution that the disk photons are Comptonized by a low-temperature ($T_{\text{e}} = 1.62_{-0.07}^{+0.10}$ keV) optically-thick ($\tau \sim 15$) material, which is clearly deviating from the very high state ($T_{\text{e}} \gtrsim 20$ keV and $\tau \lesssim 2$; Kubota & Done 2004). Recent numerical simulations anticipate that extremely high radiation pressure at a highly super-Eddington mass accretion rate ($\dot{M} \gg L_{\text{E}}/c^2$) induces a strong outflow from the disk (Ohsuga et al. 2009), which serves a cool ($T_{\text{e}} \ll 10$ keV) optically thick ($\tau \gg 1$) Comptonizing corona (Kawashima et al. 2009). Such a spectral features are gradually suggested from several high-luminosity ULXs (e.g., Gladstone et al. 2009; Vierdayanti et al. 2010). In addition, Middleton et al. (2011) applied a similar idea to the spectral variation of M33 X-8. However, the high-quality XIS spectrum from the source requires the absorption column density for the MCD+THCOMP model ($N_{\text{H}} = 0.85_{-0.14}^{+0.13} \times 10^{21} \text{ cm}^{-2}$) to be lower than the Galactic value ($N_{\text{H}} = 1.1 \times 10^{21} \text{ cm}^{-2}$; Kalberla et al. 2005). We regard such a situation invalid, considering the absorption within the M33 galaxy and intrinsic to the source. Therefore, we have concluded that the Comptonization is

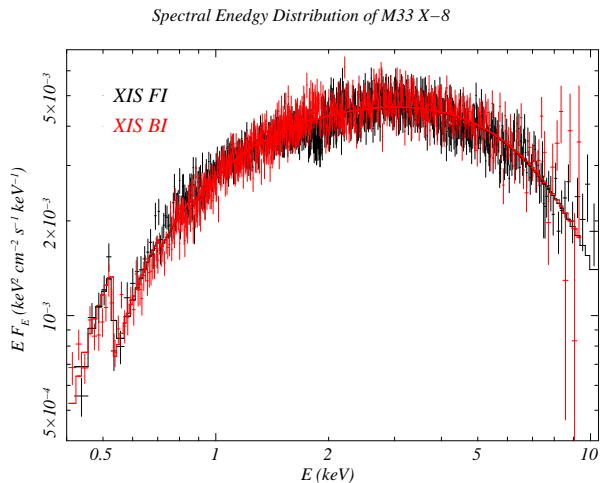


Fig. 4. Absorption-uncorrected spectral energy distribution of M33 X-8. The XIS data were de-convolved with the best-fit extended MCD model.

not a realistic scenario for M33 X-8.

4.3. Slim-disk interpretation

From observational (e.g., Kubota & Makishima 2004) and theoretical (e.g., Watarai et al. 2000) studies of Galactic black hole binaries and their accretion disk in the decade, the extended MCD model is recognized as a good approximation to the X-ray spectrum from a slim accretion disk, which is thought to be realized at a high X-ray luminosity. Actually, the model was successfully utilized to interpret the X-ray spectra of Galactic black hole binaries, at the highest end of its X-ray luminosity or in the sub-/trans-Eddington regime, as the slim disk state (e.g., XTE J1550-564; Kubota & Makishima 2004). These were subsequently followed by successful applications to the X-ray spectral properties of several ULXs (e.g., Tsunoda et al. 2006; Mizuno et al. 2007; Isobe et al. 2009).

We demonstrated that the XIS spectrum of M33 X-8 was successfully described by the extended MCD model. The innermost disk temperature and radial temperature gradient, $T_{\text{in}} = 2.00^{+0.06}_{-0.05}$ keV and $p = 0.535^{+0.004}_{-0.005}$ respectively, were both found to agree fairly with those previously inferred from the object ($T_{\text{in}} = 1.4 - 2.5$ keV and $p = 0.50 - 0.56$; Weng et al. 2009). Especially, the flat radial temperature distribution within the disk agrees with the prediction from the slim-disk theory (Watarai et al. 2000). Therefore, the slim-disk picture seems convincing for the source.

Different from Galactic black hole binaries in the classical high/soft state, which have been observationally recognized to harbor a standard accretion disk extending down to the innermost stable circular orbit at $3R_S$, a mass estimation from the assumption of $R_{\text{in}} = 3R_S$ dose not hold for a black hole with a slim disk, where R_S is the Schwarzschild radius. This is because theoretical simulations on the slim disk widely predict that emission from the accretion flow inside the innermost stable circular orbit becomes not negligible (Watarai et al. 2000). In rela-

tion, apparent dependence of the innermost disk radius (and hence the luminosity) upon the disk temperature is suggested from the numerical simulation (Watarai et al. 2000) as $R_{\text{in}} \sim T_{\text{in}}^{-1}$ (corresponding to $L_{\text{disk}} \sim T_{\text{in}}^2$). Similar properties were actually observed from several ULXs within the framework of the standard MCD+PL spectral modeling (e.g., Mizuno et al. 2001).

In order to cope with this problem, Vierdayanti et al. (2008) proposed a simple method. They fitted the numerically simulated X-ray spectra of a slim disk to the extended MCD model. They found from some representative values of black hole mass, $M = (10 - 100)M_{\odot}$, and accretion rate, $\dot{M} = (1 - 1000)L_E/c^2$, that a correction factor needs to be applied to convert the apparent mass M_X derived from the hypothesis of $R_{\text{in}} = 3R_S$ to the true one as $M/M_X = 1.2 - 1.6$. Here, we follow the technique to estimate the black hole mass of M33 X-8, assuming that the object accompanies a slim accretion disk.

The innermost disk radius of M33 X-8, $R_{\text{in}} = 81.9^{+5.9}_{-6.5}(\cos i)^{-0.5}$ km (here and hereafter dependence on κ and ξ is neglected for clarity), measured from the XIS spectrum with the extended MCD fitting gives the apparent black hole mass as $M_X = (9.2 \pm 0.7)(\cos i)^{-0.5}M_{\odot}$. Adopting the conversion factor of $M/M_X \sim 1.2$ (for $M = 10M_{\odot}$; Vierdayanti et al. 2008), the true mass of M33 X-8 is estimated as $M \sim 11(\cos i)^{-0.5}M_{\odot}$. Since the mass corresponds to the Eddington luminosity of $L_E \sim 1.7 \times 10^{39}(\cos i)^{-0.5}$ ergs s^{-1} , the source is indicated to shine at the sub-Eddington luminosity of $L_X/L_E \sim 0.4(\cos i)^{-0.5}$ or $L_{\text{disk}}/L_E \sim 0.8(\cos i)^{-0.5}$. Considering the observational fact that the Galactic black hole binaries are known to exhibit the slim-disk-like X-ray properties typically at the Eddington ratio of $L_X/L_E = 0.3 - 1$ (e.g., Kubota & Makishima 2004; Kubota et al. 2001a), the slim-disk interpretation is thought to become self-consistent for M33 X-8.

A number of authors (e.g., Okajima et al. 2006; Vierdayanti et al. 2006; Yoshida et al. 2010) utilized the X-ray model spectrum from a slim accretion disk generated from the numerical simulation by Kawaguchi (2003)³ to claim a super-Eddington interpretation for several ULXs, including M33 X-8 (Foschini et al. 2006). These have driven us to investigate the XIS spectrum with this model. The model takes into account the effects of electron scattering and general relativity in detail (with the parameter Model ID set at 7). We have to note that only the face-on disk geometry ($i = 0$) is supposed in the model. By leaving free M , \dot{M} and the viscosity parameter α , the model yielded a reasonable fit ($\chi^2/\text{dof} = 1516.7/1372$) as shown in the panel (h) of figure 3. The physical quantities derived from the slim disk model are tabulated in table 3. The black-hole mass, $M = 13.1^{+0.8}_{-0.7}M_{\odot}$, was found to nearly agree with the result from the extended MCD model. The model requires the viscosity parameter of $\alpha = 0.21 \pm 0.05$, which is not deviating far from that usu-

³ This model is available in the form compatible with XSPEC from the following web <http://heasarc.gsfc.nasa.gov/docs/xanadu/xspec/models/slimdisk.html>.

ally adopted for ULXs ($\alpha = 0.1$; e.g., Vierdayanti et al. 2006; Yoshida et al. 2010). Foschini et al. (2006) reported to prefer a lower mass of $M < 10M_{\odot}$, by applying the same model to the XMM-Newton spectra of M33 X-8 obtained in the three occasions. However, we regard that their result is possibly an artifact due to a rather low value of the disk viscosity ($\alpha < 0.01$) adopted in their analysis. It is important to note that the luminosity of the ULX is indicated to be significantly less than the Eddington limit as $L_X/L_E \sim 0.3$ or $L_{\text{disk}}/L_E \sim 0.5$, even though the source is suggested to be accreting at a super Eddington rate as $\dot{M} = 10.5_{-0.7}^{+0.5} L_E/c^2$.

We regard these results as basically supportive of the slim disk idea with the sub-Eddington luminosity for M33 X-8. However, we have to be careful about a few theoretical and observational uncertainties. The black hole mass derived from the extended MCD model is subject to the ambiguity in the spectral hardening factor κ . The numerical model on the slim accretion disk (Kawaguchi 2003) is recommended to be calibrated by the Galactic black hole binaries with a known mass, although they are known to exhibit rarely the slim disk properties. In addition, it is expected from recent numerical studies (e.g., Ohsuga et al. 2009; Kawashima et al. 2009) that the slim disk tends to accompany a strong outflow. The X-ray spectrum from the slim disk is possible to be contaminated from Comptonized X-ray photons produced in the outflow.

5. Implication to the nature of the ULXs

By making most of the Suzaku XIS spectrum with the highest signal quality ever recorded, we propose the slim disk scenario for the nearest ULX, M33 X-8. In addition, both the empirical extended MCD model and the complicated numerical simulation on the slim accretion disk have guided us to the conclusion that the source hosts a black hole with a mass of $M \gtrsim 10M_{\odot}$ (for $i = 0$). If the disk viewing angle is taken into consideration, the mass will become larger as $\propto (\cos i)^{-0.5}$ in the simplest manner neglecting the effects of the general relativity. One of the most remarkable points from this investigation is that the source is found to be radiating at the sub-Eddington luminosity, in spite of its super-Eddington mass accretion rate. A similar observational support was revealed by Isobe et al. (2009), to the sub- or trans-Eddington luminosity from the slim accretion disk by analyzing the Suzaku data for the ULX, Source 3 in the nearby galaxy NGC 2403.

A sub/trans-Eddington luminosity is not surprising from the theoretical point of view, even in the case of the super critical accretion flow ($\dot{M} \gg L_E/c^2$), since the luminosity tends to saturate due to strong advection and photon trapping. Actually, a disk luminosity of $L_{\text{disk}}/L_E \sim 3$ at most was anticipated from the numerical simulation on the slim disk at the significantly super critical accretion rate as $\dot{M} = 1000L_E/c^2$ (e.g., Vierdayanti et al. 2008). In summary, we have asserted that it is not necessary to invoke the highly super-Eddington luminosity, in order to understand the ULX behavior. By extrapolating this con-

sideration to the ULXs more luminous than M33 X-8, it is natural to conclude that there are intermediate mass black holes with a mass of $M \gtrsim 100M_{\odot}$ among those with $L_{\text{disk}} \gg 10^{40}$ ergs s $^{-1}$.

The bandpass of most operating X-ray instruments limited below 10 keV frequently prevented us to disentangle clearly the degeneracy between the candidate spectral models (e.g., the slim disk or cool Comptonization model). Actually, the capability of the hard X-ray spectrum was certified by the recent Suzaku HXD detection of the hard X-rays up to ~ 20 keV from the ULX, M82 X-1 (Miyawaki et al. 2009), since the result have succeeded in specifying the source spectrum as a Comptonized emission from a black hole with a mass of $M = (100 - 200)M_{\odot}$. Moreover, even in the case that a source is confirmed to host a slim accretion disk, a hard band X-ray spectrum above 10 keV is expected to be useful to eliminate the possible uncertainty due to the contamination from the strong outflow (see §4.3). Therefore, we expect that a wide-band X-ray spectrum in the range of 0.3 – 80 keV to be derived with the next-generation Japanese X-ray observatory ASTRO-H (Takahashi et al. 2010) will be inevitably play a crucial role to settle the nature of the ULXs.

We thank the anonymous referee for her/his supportive guidance to improve remarkably the present paper. We are grateful to all the members of the Suzaku team, for the successful operation and calibration. This research is partially supported by the MEXT Grant-in-Aid for Young Scientists (B) 22740120 (N. I.).

References

- Abubekerov, M. K., Antokhina, E. A., Bogomazov, A. I., & Cherepashchuk, A. M., 2010, *Astronomy Reports*, 53, 232
- Davis, S.W., Blaes, O.M., Hubeny, I., & Turner, N.J., 2005, *ApJ*, 621, 372
- Ebisawa, K., Makino, F., Mitsuda, K., Belloni, T., Cowley, A.P., Schmidtke, P.C., & Treves, A., 1993, *ApJ*, 403, 684
- Fabbiano, G., & Trinchieri, G., 1987, *ApJ*, 315, 46
- Fender, R. P., Belloni, T. M., & Gallo, E., 2004, *MNRAS*, 355, 1105
- Foschini, L., Rodriguez, J., Fuchs, Y., Ho, L. C., Dadina, M., Di Cocco, G., Courvoisier, T. J.-L., & Malaguti, G., 2004, *A&A*, 416, 529
- Foschini, L. et al., 2006, *Advances in Space Research*, 38, 1378
- Gladstone, J.C., Roberts, T.P., & Done, C. 2009, *MNRAS*, 397, 1836
- Hynes, R.L., Steeghs, D., Casares, J., Charles, P.A., & O'Brien, K. 2003, *ApJ*, 583, L95
- Ishisaki, Y., et al. 2007, *PASJ*, 59, 113
- Isobe N., et al., 2008, *PASJ*, 60S, 241
- Isobe N., et al., 2009, *PASJ*, 61S, 279
- Kalberla, P. M. W., Burton, W. B., Hartmann, Dap, Arnal, E. M., Bajaja, E., Morras, R., & Poöppel, W. G. L., 2005, *A&A*, 440, 775
- Kawaguchi, T., 2003, *ApJ*, 593, 69
- Kawashima, T., Ohsuga, K., Mineshige, S., Heinzeller, D., Takabe, H., & Matsumoto, R., 2009, *PASJ*, 61, 769
- Koyama K., et al., 2007, *PASJ*, 59, S23
- Kubota, A., & Done, C., 2004, *MNRAS*, 353, 980

- Kubota, A., Done, C., & Makishima, K. 2002, MNRAS, 337, L11
- Kubota, A., Makishima, K., & Ebisawa, K., 2001a, ApJ, 560, L147
- Kubota, A., & Makishima, K., 2004, ApJ, 601, 428
- Kubota, A., Mizuno, T., Makishima, K., Fukazawa, Y., Kotoku, J., Ohnishi, T., & Tashiro, M., 2001b, ApJ, 547, L119
- Kubota, A., Tanaka, Y., Makishima, K., Ueda, Y., Dotani, T., Inoue, H., & Yamaoka, Y. 1998, PASJ, 50, 667
- La Parola, V., Damiani, F., Fabbiano, G., & Peres, G., 2003, ApJ, 583, 758
- Lasker, B. M., Sturch, C. R., McLean, B. J., Russell, J. L., Jenkner, H.; Shara, M. M., AJ, 99, 2019
- Makishima, K., et al., 2000, ApJ, 535, 632
- Makishima, K., Maejima, Y., Mitsuda, K., Bradt, H. V., Remillard, R. A., Tuohy, I. R., Hoshi, R., Nakagawa, M., 1986, ApJ, 308, 635
- Mineshige, S., Hirano, A., Kitamoto, S., Tamada, T. T., Fukue, J. 1994, ApJ, 426, 308
- Middleton, M.J., Sutton, A.D., & Roberts, T.P., 2011, MNRAS, 417, 464
- Mitsuda, K., et al., 2007, PASJ, 59, S1
- Miyamoto, S., Kimura, K., Kitamoto, S., Dotani, T., & Ebisawa, K., 1991, ApJ, 383, 784
- Miyawaki, R., Makishima, K., Yamada, S., Gandhi, P., Mizuno, T., Kubota, A., Tsuru, T. G., & Matsumoto, H., 2009, PASJ, 61, S263
- Mizuno, T., Kubota, A., & Makishima, K., 2001, ApJ, 554, 1282
- Mizuno, T., et al., 2007, PASJ, 59, S257
- Mitsuda, K., et al., 1984, PASJ, 36, 741
- Ohsuga, K., Mori, M., Nakamoto, T., & Mineshige, S., 2005, ApJ, 628, 368
- Ohsuga, K., Mineshige, S., Mori, M., & Kato, Y. 2009, PASJ, 61, L7,
- Okajima, T., Ebisawa, K., & Kawaguchi, T., 2006, ApJ, 652, L1050
- Parmar, A. N., 2001, A&A, 368, 420
- Serlemitsos, P.J, et al., 2007, PASJ, 59, S9
- Shahbaz, T., van der Hooft, F., Casares, J., Charles, P.A., & van Paradijs, J. 1999, MNRAS, 306, 89
- Swartz, D.A., Soria, R., Tennant, A.F., & Yukita, Mihoko 2011, ApJ, 741, 49
- Shakura N. I., & Sunyaev, R. A. 1973, A&A, 24, 337
- Shimura, T., & Takahara, F., 1995, ApJ, 445, 780
- Sunyaev, R. A., & Titarchuk, L. G., 1980, A&A, 86, 121
- Takahashi, T., et al., 2007, PASJ, 59, S35
- Takahashi, T., et al., 2010, SPIE, 7732, 27
- Takano, M., Mitsuda, K., Fukazawa, Y., & Nagase, F. 1994, ApJ, 436, 47
- Tanaka, Y., 1997, in *Accretion Disks – New Aspects, Proceedings of the EARA Workshop Held in Garching, Germany*, (Lecture Notes in Phys., 487; Springer Berlin / Heidelberg)
- Trinchieri, G., Fabbiano, G., & Peres, G., 1988, ApJ, 325, 531
- Tsunoda, N., Kubota, A., Namiki, M., Sugiho, M., Kawabata, K., & Makishima, K., 2006, PASJ, 58, 1081
- Uchiyama et al., 2008, PASJ, 60, S35
- Ueda, Y., et al., 2010, ApJ, 713, 257
- van den Bergh, S. 1991, PASP, 103, 609
- Vierdayanti, K., Done, C., Roberts, T.P., & Mineshige, S., 2010, MNRAS, 403, 1206
- Vierdayanti, K., Mineshige, S., Ebisawa, K., & Kawaguchi, T. 2006, PASJ, 58, 915,
- Vierdayanti, K., Watarai, K., & Mineshige, S., 2008, PASJ, 60, 653
- Watarai, K., Fukue, J., & Mineshige, S., 2000, PASJ, 52, 133
- Watarai, K., & Mineshige, S., 2003, ApJ, 596, 421
- Weng, S.-S., Wang, J.-X., Gu, W.-M., & Lu, J.-F., 2009, PASJ, 61, 1287
- Yoshida, T., Ebisawa, K., Matsushita, K., Tsujimoto, M., & Kawaguchi, T. 2010, ApJ, 722, 760
- Zdziarski, A. A., Johnson, W. N., & Magdziarz, P. 1999, MNRAS, 283, 193